Channel flows of shear-thinning fluids that mimic the mechanical response of a Bingham fluid

Channel flows of shear-thinning fluids that mimic the mechanical response of a Bingham fluid

Lorenzo Fusi*, Angiolo Farina

Università degli Studi di Firenze, Dipartimento di Matematica e Informatica "Ulisse Dini", Viale Morgagni 67/A, 50134 Firenze, Italy.

Kumbakonam R. Rajagopal

Texas A&M University, Department of Mechanical Engineering, 301 Olsen Blvd, College Station, TX 77845, USA

Luigi Vergori

Università degli Studi di Perugia, Dipartimento di Ingegneria, Via Goffredo Duranti 93, 06125 Perugia, Italy.

Abstract

The linear stability of channel flows driven by pressure drops is carried out for fluids that exhibit a yield stress, the mechanical response of which is prescribed by the Bingham constitutive relation or two of its regularizations: the simple model due to Allouche et al. [1] and Papanastasiou model. The critical thresholds for the onset of turbulence predicted by using the regularized models differ very slightly, while they differ significantly from the critical Reynolds number predicted for the Bingham model. We show that this discrepancy is due to the presence of a rigid core in a Bingham fluid that does not dissipate energy.

Keywords: Bingham fluids, Simple and Papanastasiou models, stability of Poiseuille flows

*Corresponding author

Email address: `lorenzo.fusi@unifi.it` (Lorenzo Fusi)

1. Introduction

Viscoplastic materials are defined through constitutive relations that contain a yield stress, namely a threshold to be breached for the fluid to start flowing. Materials exhibiting such a behavior include colloidal suspensions, muds, foams, emulsions, lava and a large variety of products employed in the food industry. The yield stress can be regarded also as a demarcation from solid-like to fluid-like behavior. In practice, below the critical threshold the micro-structure of the material is rigid enough to resist to any stress smaller than the yield limit. In viscoplastic materials, the behavior below the yield stress is actually that of a deformable solid in which the rate of deformation is so small that it can be neglected. In this perspective, the notion of viscoplastic material is, as a matter of fact, an idealization. In other words we can state that below the critical limit the deformation is so "small" that we may consider the material as an undeformable rigid body.

The assumption of rigidity implies that the constitutive relation is singular at zero shear-rate, with the stress being indeterminate below the critical threshold. This implies that the stress-shear rate relation is a graph and not a one-to-one mapping. Recently, this problem has been circumvented by assuming the rate of strain as a function of the stress [12], [13].

The simplest (and probably the most widely used) viscoplastic constitutive relation is the Bingham constitutive relation. In this model, the relation between the stress and the symmetric part of the velocity gradient is linear above the yield limit [3]. More complex constitutive equations can be adopted for describing the fluid behavior of the material (the Herschel-Bulkley and Casson models, to cite two of them). The use of viscoplastic models is mathematically attractive although it poses several analytical and numerical issues. Indeed, being an idealization, viscoplastic models may lead to results with unclear physical interpretations and, in some circumstances, also paradoxes [5, 6]. A way to overcome these issues is to use regularized models that approximate the viscoplastic response without introducing the notion of a yield stress. Typically, these regularized models depend on a positive parameter which accounts for the accuracy of the approximation.

Of course, models approximating the Bingham constitutive relation can be chosen quite arbitrarily. The simple model due to Allouche et al. [1], the models due to Bercovier-Engelman [2] and Papanastasiou [14] are three of the most widely used regularizations of the relation between the symmetric part of the velocity gradient and the stress for a yield stress fluid. Very recently Garimella et al. [9] have proposed a new class of fluids that mimic viscoplastic behavior, in which the stress that the fluid can sustain is bounded. Here we study the linear stability of Poiseuille flows in a viscoplastic material by adopting the Bingham, simple and Papanastasiou models. In particular, we shall show the differences in the critical thresholds for the Reynolds number when using models with and without a yield stress. The critical thresholds for the onset of instability in regularized models do not coincide with that of the exact Bingham model. Such a discrepancy in the critical thresholds for the onset of instability has been observed also in different flow regimes [8, 11]. We shall show how the discrepancy in the critical thresholds for the Reynolds number is a consequence of the hypothesis of perfect rigidity of the unyielded domain. Indeed, the absence of deformation does not allow the rigid core to undergo any kind of perturbation and hence to dissipate energy, while in the regularized case energy is dissipated throughout the domain occupied by the fluid. To prove this assertion, we shall study the linear stability by removing the region corresponding to the unyielded phase in a Bingham fluid from the domain over which the evolution equation of perturbations for a regularized model has to be solved, and find out that, in doing so, the critical thresholds for the Reynolds number coincide.

2. The Bingham model and some of its regularizations

According to the Bingham model for the mechanical response of an incompressible viscoplastic material, the stress tensor results in the sum of an arbitrary spherical part $-p^*\mathbf{I}$, with p^* being the Lagrange multiplier associated with the constraint of incompressibility and having the same physical dimensions as the pressure, and an extra stress $\mathbf{S}^*$ related to the rate of strain tensor $\mathbf{D}^* = [\nabla^*\mathbf{v}^* + (\nabla^*\mathbf{v}^*)^T]/2$, with $\mathbf{v}^*$ being the velocity field, according to

$$\begin{cases} \mathbf{S}^* = \left(2\mu^* + \dfrac{\tau_0^*}{|\mathbf{D}^*|}\right)\mathbf{D}^*, & \text{if } |\mathbf{S}^*| \geq \tau_0^*, \\ \mathbf{D}^* = 0 & \text{if } |\mathbf{S}^*| \leq \tau_0^*, \end{cases} \tag{1}$$

where $\mu^* > 0$ is the plastic viscosity, and $\tau_0^* > 0$ is the yield stress.

Throughout this paper, given a second-order tensor $\mathbf{A}$ with components A_{ij} $(i, j = 1, 2, 3)$, $|\mathbf{A}|$ is the non-negative scalar $|\mathbf{A}| = \sqrt{\frac{1}{2}\mathbf{A}\cdot\mathbf{A}} = \sqrt{\frac{1}{2}\sum_{i,j=1}^{3} A_{ij}^2}$. Observe that, if $\mathbf{A}$ is symmetric and traceless (like $\mathbf{D}^*$ and $\mathbf{T}^*$), $|\mathbf{A}|$ is the negative of the second principal scalar invariant of $\mathbf{A}$.

There are many ways to regularize the Bingham model. In this manuscript we shall consider two of them: the simple model[1]

$$\mathbf{S}^* = \left(2\mu^* + \frac{\tau_0^*}{|\mathbf{D}^*| + \varepsilon^*}\right)\mathbf{D}^*, \tag{2}$$

and the Papanastasiou model

$$\mathbf{S}^* = \left\{2\mu^* + \frac{\tau_0^*\left[1 - \exp\left(-|\mathbf{D}^*|/\varepsilon^*\right)\right]}{|\mathbf{D}^*|}\right\}\mathbf{D}^*. \tag{3}$$

The positive parameter ε^* occurring in (2) and (3) has the same physical dimensions as the shear-rate.

2.1. Basic equations

We shall consider flows between two parallel plates of length L^* in one direction and infinite in the other located at distance $2H^*$ from each other. For convenience, we introduce a Cartesian frame of reference $Ox^*y^*z^*$ with unit vectors $\mathbf{i}$, $\mathbf{j}$ and $\mathbf{k}$ such that the parallel plates occupies the strips $S_\pm = \{(x^*, y^*, z^*) \in \mathbb{R}^3 : x^* \in [0, L^*],\ y^* = \pm H^*\}$. In the absence of body forces, the constraint of

[1] Throughout the paper we denote with "simple model" the constitutive relation due to Allouche et al. [1].

incompressibility and the equation of balance of linear momentum read

$$\begin{cases} \operatorname{div}^* \mathbf{v}^* = 0, \\ \\ \rho^* \dot{\mathbf{v}}^* = -\nabla^* p^* + \operatorname{div}^* \mathbf{S}^*, \end{cases} \tag{4}$$

where ρ^* is the (constant) mass density of the fluid and the superposed dot denotes the material time derivative.

When adopting the Bingham model for describing the mechanical response of a viscoplastic material, the equations of balance (4) hold only in the yielded region, that we identify with the region in which $|\mathbf{S}^*| \geq \tau_0^*$. Instead, the motion of the unyielded region is rigid. Thus, the equation of balance of linear momentum has to be written in integral form. In analogy with the unyielded domain, we identify the inner rigid core with the non-material region $\Omega^*_{t^*}$ in which $|\mathbf{S}^*| \leq \tau_0^*$.

The equation of balance of linear momentum over $\Omega^*_{t^*}$ reads

$$\int_{\Omega^*_{t^*}} \varrho^* \left[\frac{\partial \mathbf{v}^*}{\partial t^*} + \operatorname{div} \Big(\mathbf{v}^* \otimes \mathbf{v}^* \Big) \right] dV^* = \int_{\partial \Omega^*_{t^*}} \mathbf{T}^* \mathbf{n} \, dA^*, \tag{5}$$

where $\mathbf{n}$ is the unit outward normal to $\partial\Omega^*_{t^*}$, and, in view of Newton's third law, the stress $\mathbf{T}^*$ is the same as that in the yielded domain.

For plane flows of the form $\mathbf{v}^* = u^*(x^*, y^*, t^*)\mathbf{i} + v^*(x^*, y^*, t^*)\mathbf{j}$, with u^* and v^* symmetric about the x^* axis, the inner core takes the simple form

$$\Omega^*_{t^*} = \Big\{ (x^*, y^*, z^*) \in \mathbb{R}^3 : \; x^* \in [0, L^*], \; y^* \in [-s^*(x^*, t), s^*(x^*, t)] \Big\},$$

where the boundaries $y^* = \pm s^*(x^*, t)$ represent the yield surfaces. In this flow regime, by following similar arguments as in [4], one can prove that the integral equation of balance (5) leads to the scalar equation

$$\begin{aligned} \varrho^* \dot{u}^*_c \int_0^{L^*} s^* dx^* = & \int_0^{L^*} S_{12}|_{y^*=s^*(x^*,t^*)} \, dx^* \\ & - \int_0^{L^*} \left[s^* \frac{\partial}{\partial x^*} \Big(p^*|_{y^*=s^*(x^*,t^*)} \Big) + \frac{\partial s^*}{\partial x^*} S^*_{11} \right]_{y^*=s^*(x^*,t^*)} dx^*, \end{aligned} \tag{6}$$

where $\mathbf{v}^*_c = u^*_c(t^*)\mathbf{i}$ is the velocity of the rigid core.

2.2. Nondimensionalization

In what follows we shall be interested in isochoric parallel shear flows that are driven by a given pressure drop $\Delta p^* = p^*_{in} - p^*_{out} > 0$ in x^*-direction. It is then convenient to non-dimensionalize the governing equations by introducing the following dimensionless quantities

$$\begin{aligned} &\mathbf{x} = \frac{\mathbf{x}^*}{H^*}, \quad \mathbf{v} = \frac{\mathbf{v}^*}{U^*}, \quad t = \frac{U^*}{H^*}t^*, \quad p = \frac{p^* - p^*_{out}}{\Delta p^*}, \\ &s = \frac{s^*}{H^*}, \quad u_c = \frac{u^*_c}{U^*}, \quad \mathbf{D} = \frac{H^*}{U^*}\mathbf{D}^*, \quad \mathbf{S} = \frac{H^*}{\mu^* U^*}\mathbf{S}^*, \end{aligned} \tag{7}$$

where U^* is a reference speed to be chosen suitably.

Introducing (7) into the governing equations (4) and (6) yields

$$\begin{cases} \mathrm{div}\mathbf{v} = 0, \\ \\ Re\dot{\mathbf{v}}^* = -Re\, Eu \nabla p + \mathrm{div}\mathbf{S}, \end{cases} \tag{8}$$

and

$$\begin{aligned} Re\dot{u}_c \int_0^\delta s dx = &\int_0^\delta S_{12}\big|_{y=s(x,t)} dx \\ &- \int_0^\delta \left[Re\, Eu\, s \frac{\partial}{\partial x}\left(p\big|_{y=s(x,t)}\right) + \frac{\partial s}{\partial x} S_{11} \right]_{y=s(x,t)} dx, \end{aligned} \tag{9}$$

where

$$Re = \frac{\varrho^* U^* H^*}{\mu^*} \quad \text{and} \quad Eu = \frac{\Delta p^*}{\rho^* U^{*2}} \tag{10}$$

are the Reynolds and Euler numbers, respectively and $\delta = L^*/H^*$.

As the nondimensionalization of the constitutive relations is concerned, inserting (7) into (1), (2) and (3), and introducing the Bingham number, $Bi = \tau^*_0 H^*/(\mu^* U^*)$, yield

$$\mathbf{S} = \underbrace{\left(2 + \frac{Bi}{|\mathbf{D}|}\right)}_{\mu_B(|\mathbf{D}|)} \mathbf{D} \quad \text{if } |\mathbf{S}| \geq Bi, \tag{11}$$

for the Bingham model,

$$\mathbf{S} = \underbrace{\left(2 + \frac{Bi}{|\mathbf{D}| + \varepsilon/2}\right)}_{\mu_S(|\mathbf{D}|)} \mathbf{D}, \tag{12}$$

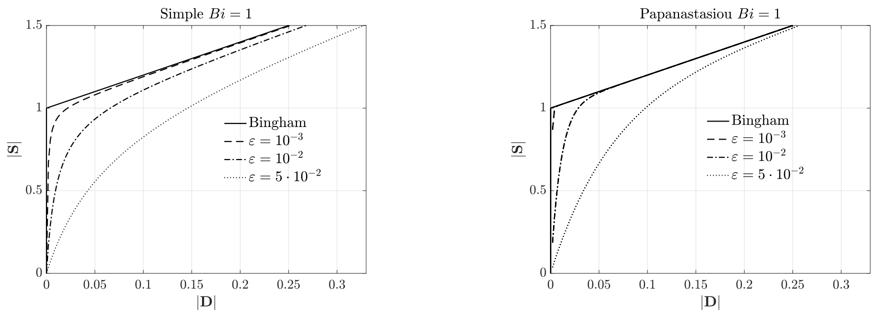

(a) Simple model. (b) Papanastasiou model.

Figure 1: Constitutive relation due to Allouche et al. [1] and Papanastasiou [14] for different values of ε. It is evident that both of them tend to the Bingham model as ε tends to zero.

for the simple model, and

$$\mathbf{S} = \underbrace{\left\{ 2 + \frac{Bi\left[1 - \exp\Big(-2|\mathbf{D}|/\varepsilon\Big)\right]}{|\mathbf{D}|} \right\}}_{\mu_P(|\mathbf{D}|)} \mathbf{D}, \tag{13}$$

for the Papanastasiou model.

In (12) and (13) we have set $\varepsilon = 2\varepsilon^* L^*/U^*$. In the limit as $\varepsilon \to 0^+$, the dimensionless regularized models (12) and (13) tend to the dimensionless Bingham model (11). To unveil such an asymptotic behaviour, we take the norm of both sides of equations (11), (12) and (13), and plot $|\mathbf{S}|$ versus $|\mathbf{D}|$ for different values of ε (figure 1).

3. Poiseuille flows

As anticipated in the previous section, here we are interested in steady laminar flows of the form $\mathbf{v} = u(y)\mathbf{i}$ that are generated by a pressure drop in x-direction (i.e. Poiseuille flows). For these flows, it easy to check that $D_{12} = u'(y)/2$ (with the prime denoting differentiation with respect to y) is the only non-zero component of the symmetric part of the velocity gradient, by which it immediately follows that S_{12} is the only non-vanishing component of the extra stress and, depending on the constitutive model used, it is given by

$$S_{12} = \left(1 + \frac{Bi}{|u'|}\right) u' \quad \text{if} \quad |S_{12}| \geq Bi, \tag{14}$$

for the Bingham model,

$$S_{12} = \left(1 + \frac{Bi}{|u'| + \varepsilon}\right) u', \tag{15}$$

for the simple model, and

$$S_{12} = \left\{1 + \frac{Bi\Big[1 - \exp\left(-|u'|/\varepsilon\right)\Big]}{|u'|}\right\} u', \tag{16}$$

for the Papanastasiou model.

Next, from $(8)_2$, within the nondimensionalization adopted, the Lagrange multiplier associated with the constraint of incompressibility is found to be $p = (\delta - x)/\delta$, so that the equation governing the Poiseuille flows reads

$$S_{12}' = -G, \tag{17}$$

where $G = Re\, Eu/\delta$ is the dimensionless pressure gradient.

Equation (17), with the shear stress S_{12} as in (14), (15) or (16), and supplemented with the no-slip boundary conditions $u(\pm 1) = 0$, can be solved analytically. Specifically, we have

- for the Bingham model

$$u_B(y) = \begin{cases} \dfrac{(Bi - G)^2 - (Bi - G|y|)^2}{2G} & \text{if } |y| \in [s_B, 1], \\[2ex] \dfrac{(Bi - G)^2}{2G} & \text{if } |y| \in [0, s_B], \end{cases} \tag{18}$$

  with $s_B = Bi/G$;

- for the simple model

$$\begin{aligned} u_S(y) = {} & \frac{(Bi + \varepsilon - G)^2 - (Bi + \varepsilon - G|y|)^2}{4G} \\ & - \frac{\varepsilon Bi}{G}\Bigg\{\xi(1)\sqrt{\xi^2(1) + 1} + \operatorname{settsinh}[\xi(1)] \\ & - \xi(|y|)\sqrt{\xi^2(|y|) + 1} - \operatorname{settsinh}[\xi(|y|)]\Bigg\}, \end{aligned} \tag{19}$$

where η is such that

$$\xi : s \in [0,1] \mapsto \frac{Gs - Bi + \varepsilon}{2\sqrt{\varepsilon Bi}}; \tag{20}$$

- for the Papanastasiou model

$$\begin{aligned} u_P(y) = {} & \frac{(Bi-G)^2 - (Bi - G|y|)^2}{2G} \\ & - \frac{\varepsilon^2}{2G}\left\{ \Big[\mathrm{W}_0(\zeta(1)) + 1\Big]^2 - \Big[\mathrm{W}_0(\zeta(|y|)) + 1\Big]^2 \right\}, \end{aligned} \tag{21}$$

where W_0 is the principal branch of the Lambert function [10], and ζ is defined as

$$\zeta : s \in [0,1] \mapsto \frac{Bi}{\varepsilon} \exp\left[\frac{Bi}{\varepsilon}\left(1 - \frac{G|y|}{Bi}\right)\right]. \tag{22}$$

Observe that in a Bingham material the Poiseuille flow (18) happens only if the dimensionless pressure gradient exceeds the Bingham number, or, equivalently, if $\Delta p^* H^* > \tau_0^* L^*$.

In the previous section we have mentioned that the reference speed U^* has to be chosen suitably. Indeed, it is convenient to take U^* such that the dimensionless velocity has maximum modulus equal to unity. This is equivalent to choosing as the reference speed the value of U^* for which $u_o(0) = 1$ ($o = B, S, P$).

For Bingham materials it is easy to check that one has to take $U^* = (\Delta p^* H^* - \tau_0^* L^*)^2 / (2\Delta p^* L^* \mu^*)$ in order to have $u_B(0) = 1$. With this choice of the reference speed, the solution to Poiseuille flow (18) becomes

$$u_B(y) = \begin{cases} 1 - \left(\dfrac{|y| - s_B}{1 - s_B}\right)^2 & \text{if } |y| \in [s_B, 1], \\ 1 & \text{if } |y| \in [0, s_B]. \end{cases} \tag{23}$$

When using the simple and Papanastasiou models the value of U^* for which the maximum speed is equal to unity can be determined only numerically.

We finally observe that the velocity profiles (19) and (21) tend to (23) as $\varepsilon \to 0$. To highlight this asymptotic behaviour, figures 2 and 3 display the velocity profiles u_k ($k = S, P$) at different values of ε for $Bi = 1$ and $Bi = 7$,

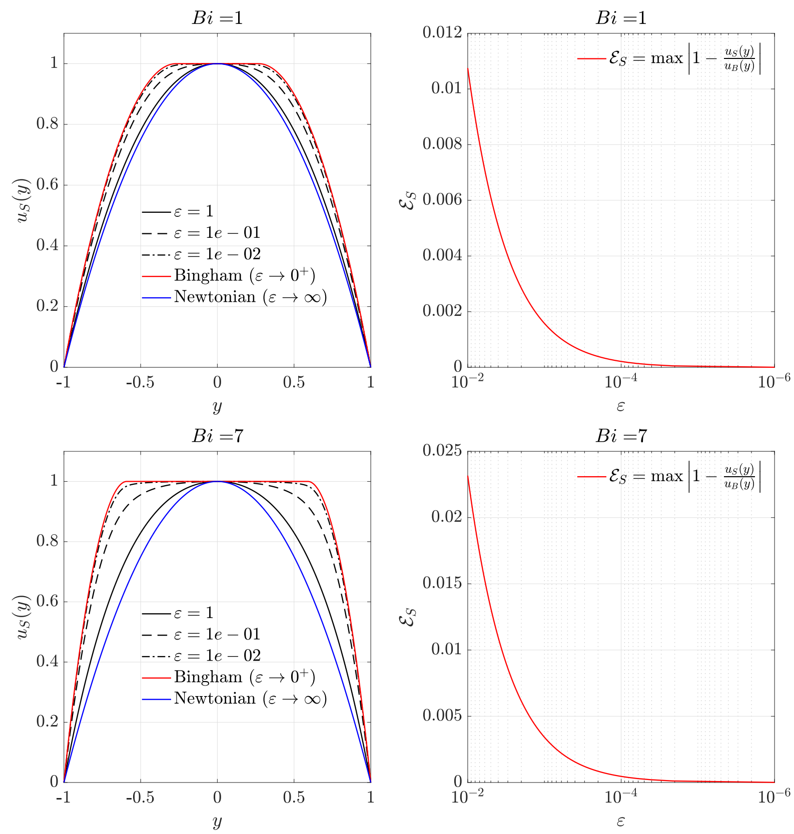

Figure 2: Velocity profiles and maximum relative error when using the simple model.

and the maximum relative errors in using the simple and Papanastasiou models instead of the 'exact' Bingham model,

$$\mathcal{E}_k(\varepsilon) = \max_{y\in[-1,1]} \left|1 - \frac{u_k(y;\varepsilon)}{u_B(y)}\right| \quad (k = S, P),$$

as functions of ε.

3.1. The Bingham and Reynolds numbers

We observe that the Bingham number Bi is a "flow dependent" quantity as it depends on the characteristic speed. On the other hand, we can re-write it as

$$Bi = \frac{\tau_0^* L^*}{\mu^* U^*} = \frac{1}{Re}\left(\frac{\tau_0^* {L^*}^2 \varrho^*}{{\mu^*}^2}\right) = \left(\frac{\tau_0^*}{Re\,\sigma^*}\right), \quad \text{with} \quad \sigma^* = \frac{{\mu^*}^2}{\varrho^* {L^*}^2}, \tag{24}$$

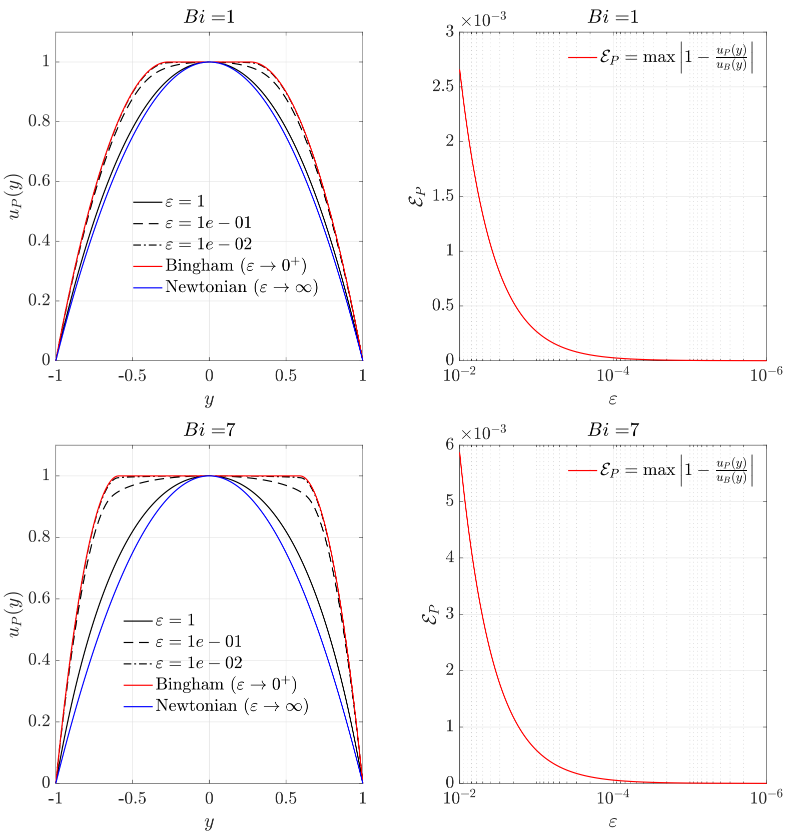

Figure 3: Velocity profiles and maximum relative error when using the Papanastasiou model.

where $Re\,\sigma^*$ is the characteristic viscous stress, with σ^* being a sort of characteristic viscous stress per unit Reynolds number, and τ_0^* is the yield stress.

We now introduce the quantity

$$\Gamma = \frac{\tau_0^*}{\sigma^*} = \frac{\tau_0^* {L^*}^2 \varrho^*}{{\mu^*}^2}, \tag{25}$$

which coincides with the Bingham number when $Re = 1$. Clearly, Γ depends only on material and geometrical parameters and allows us to write the Bingham numer in terms of the Reynolds number:

$$Bi = \frac{\Gamma}{Re}. \tag{26}$$

When dealing with linear modal stability - in which critical conditions are sought varying the Reynolds number - it makes more sense to use (26) with Γ fixed than treating Bi and Re as independent quantities as it is often done in the literature (see, for instance, [7]). It is because of this that, in order to compare our results with those existing in the literature, we shall perform the stability analysis by considering both the case in which Bi and Re are independent from each other, and the case in which Γ is fixed and the Bingham and Reynolds numbers are related through (26).

4. Linear stability analysis

We now study the linear stability of the Poiseuille flows (19), (21) and (23). To this end, we introduce a two-dimensional perturbation to the basic solution $(u_o\mathbf{i}, p_o = (\delta - x)/\delta)$, with $o = B, S, P$, in the form of a travelling wave in the x-direction,

$$\mathbf{v} = u_o(y)\mathbf{i} + \hat{\mathbf{u}}(y) \exp\Big[i\alpha(x - ct)\Big], \quad p = \frac{\delta - x}{\delta} + \frac{\hat{p}(y)}{\delta} \exp\Big[i\alpha(x - ct)\Big], \tag{27}$$

where $\hat{\mathbf{u}} = \hat{u}\mathbf{i} + \hat{v}\mathbf{j}$, α is the wave number (real), and $c = c_r + ic_i$ is the (complex) wave speed. Inserting (27) into the governing equations (8) and linearising we obtain

$$\begin{cases} i\alpha\hat{u} + \hat{v}' = 0, \\ Re\Big[- i\alpha c\hat{u} + u_o'\hat{v} + i\alpha u_o\hat{u}\Big] = -i\alpha G\hat{p} + i\alpha\hat{S}_{11} + \hat{S}_{12}', \\ Re\Big[- i\alpha c\hat{v} + i\alpha u_o\hat{v}\Big] = -G\hat{p}' + i\alpha\hat{S}_{12} + \hat{S}_{22}', \end{cases} \tag{28}$$

where

$$\hat{S}_{11} = i\alpha\mu_o(|u_o'|/2)\hat{u}, \quad \hat{S}_{22} = \mu_o(|u_o'|/2)\hat{v}',$$

$$\hat{S}_{12} = \underbrace{\frac{1}{2}\left[\mu_o(|u_o'|/2) + \frac{|u_o'|}{2}\frac{d\mu_o}{d|\mathbf{D}|}(|u_o'|/2)\right]}_{\equiv f_o(|u_o'|/2)}(\hat{u}' + i\alpha\hat{v}). \tag{29}$$

On replacing $\hat{u}$ with $-\hat{v}'/(i\alpha)$ (c.f. $(28)_1$) and eliminating the pressure in $(28)_2$ and $(28)_3$, the evolution equations of perturbations reduce to the single ordinary differential equation

$$\begin{aligned} & h_o\Big(\mathsf{D}^2 - \alpha^2\Big)^2\hat{v} - i\alpha Re\Big[(u_o - c)(\mathsf{D}^2 - \alpha^2) - u_o''\Big]\hat{v} \\ & = -\Big\{(2h_o')\mathsf{D}^3 + \big[2\alpha^2(2h_o - g_o) + h_o''\big]\mathsf{D}^2 + 2\alpha^2(h_o' - g_o')\mathsf{D} + \alpha^2 h_o''\Big\}\hat{v}, \end{aligned} \tag{30}$$

where $g_o(y) = \mu(|u_o'(y)|/2)$, $h_o(y) = f_o(|u_o'(y)|/2)$, and D is the differential operator $\dfrac{d}{dy}$.

Equation (30) is a generalization of the Orr-Sommerfeld equation. In particular, it reduces to the Orr-Sommerfeld equation when the Bingham number vanishes.

Like the Orr-Sommerfeld equation, (30) must be supplemented by appropriate boundary conditions. When dealing with the regularized models (12) and (13), these conditions are

$$\hat{v}(\pm 1) = \hat{v}'(\pm 1) = 0. \tag{31}$$

Instead, when dealing with the Bingham model, since equation (30) has to be solved over the domain $[-1, -s_B] \cup [s_B, 1]$, two boundary conditions on each yield plane, i.e. at $y = \pm s_B$, must be added to (31).

4.1. The Bingham case

In this case the basic solution is as in (23). In view of the symmetry of the problem, we may limit our analysis to the domain $[0, 1]$.

On the perturbed yield surface $y = s_B + \hat{s}e^{i\alpha(x-ct)}$ (with $\hat{s} = const$) (and everywhere within the unyielded phase) the longitudinal velocity is a function of time only, while the transverse velocity and the symmetric part of the velocity gradient must vanish. We have then

$$u\Big|_{y=s_B+\hat{s}e^{i\alpha(x-ct)}} = u_c, \quad v\Big|_{y=s_B+\hat{s}e^{i\alpha(x-ct)}} = 0, \quad \mathbf{D}\Big|_{y=s_B+\hat{s}e^{i\alpha(x-ct)}} = 0, \quad (32)$$

which, once linearised, yield

$$\hat{u}(s_B) = \hat{v}(s_B) = \hat{v}'(s_B) = 0, \quad \text{and} \quad \frac{2\hat{s}}{1-s_B} = \hat{u}'(s_B). \quad (33)$$

We now introduce the perturbed fields into the integral equation of balance (9). After linearisation, we obtain

$$\int_0^\delta \Big[\underbrace{S'_{12}(s_B)}_{=-G}\hat{s} + \hat{S}_{12}(s_B) + G\hat{s} - i\alpha G s_B \hat{p}\Big] e^{i\alpha(x-ct)}dx = 0, \quad (34)$$

which, in view of $(28)_2$, $(29)_3$ and (33), yields the boundary condition $(1 - s_B)\hat{u}'(s_B) = 0$. Hence, since Poiseuille flows happen in a Bingham fluid only if $s_B < 1$, we have $\hat{u}'(s_B) = 0$, and, as an immediate consequence of the last condition in (33), we deduce that $\hat{s} = 0$. This means that the rigid unyielded region is not affected by infinitesimal perturbations.

Summarising, the components $\hat{u}$ and $\hat{v}$ of the perturbation to the basic flow must satisfy the following boundary conditions on the yield planes $y = \pm s_B$:

$$\hat{u}(\pm s_B) = \hat{u}'(\pm s_B) = \hat{v}(\pm s_B) = \hat{v}'(\pm s_B) = 0. \quad (35)$$

We are now in position to solve the eigenvalue problem given by (30), (31) and (35) for the Bingham case, i.e. for $o = B$. In this case, we have

$$g_B = 2\left(1 + \frac{Bi}{|u'_B|}\right) \quad \text{and} \quad h_B = 1, \quad (36)$$

with u_B as in (23), so that equation (30) becomes

$$\left(\mathsf{D}^2-\alpha^2\right)^2\hat{v}-i\alpha Re\Big[(u_B-c)(\mathsf{D}^2-\alpha^2)-u_B''\Big]\hat{v}=4\alpha^2 Bi\mathsf{D}\left(\frac{\mathsf{D}\hat{v}}{|u_B'|}\right), \qquad (37)$$

which coincides with the perturbation equation for Poiseuille flows in Bingham fluids obtained in previous studies [3], [7].

We solve this eigenvalue problem numerically by using a spectral collocation method based on Chebyshev polynomials. Therefore, as a first step, we map the domain $[-1,-s_B]\cup[s_B,1]$ into $[-1,1]$ on using the transformation

$$\bar{\eta}: y\in[-1,-s_B]\cup[s_B,1]\mapsto \eta=\mathrm{sign}(y)\frac{|y|-s_B}{1-s_B}\in[-1,1]. \qquad (38)$$

The problem is thus reformulated for $\bar{v}(\eta)=\hat{v}(y)$. With this change of variables, equation (37) becomes

$$\left(\lambda^2\mathcal{D}^2-\alpha^2\right)^2\bar{v}-i\alpha Re\Big[(1-\eta^2-c)(\lambda^2\mathcal{D}^2-\alpha^2)+2\lambda^2\Big]\bar{v}=2\alpha^2\lambda Bi\mathcal{D}\left(\frac{\mathcal{D}\bar{v}}{|\eta|}\right), \quad (39)$$

where

$$\bar{v}(\eta)=\hat{v}(\bar{\eta}^{-1}(\eta)), \quad \mathcal{D}=\frac{d}{d\eta}, \quad \mathsf{D}^n=\mathcal{D}^n\frac{1}{(1-s_B)^n}\equiv\lambda^n\mathcal{D}^n \quad (n\in\mathbb{N}), \quad (40)$$

while the boundary conditions (31) and (35) collapse to

$$\bar{v}(\pm1)=\mathcal{D}\bar{v}(\pm1)=0. \qquad (41)$$

Observe that, in view of the boundary conditions on the yield planes (35) and the incremental constraint of incompressibility $(28)_1$, it can be shown that the singularity in the right hand side of (39) is only apparent and $\mathcal{D}\bar{v}/|\eta|\to 0$ as $\eta\to 0$.

It is worth noting also that when the Bingham number vanishes, $\lambda=1$ and (39) reduces to the classical Orr-Sommerfeld equation.

The eigenvalue problem problem (39)-(41) has been solved using a spectral collocation method based on Chebyshev polynomials with $N=200$ Gauss-Lobatto points. The classic Orr-Sommerfeld problem (Newtonian fluids) has been used as a benchmark to guarantee the reliability of the numerical code.

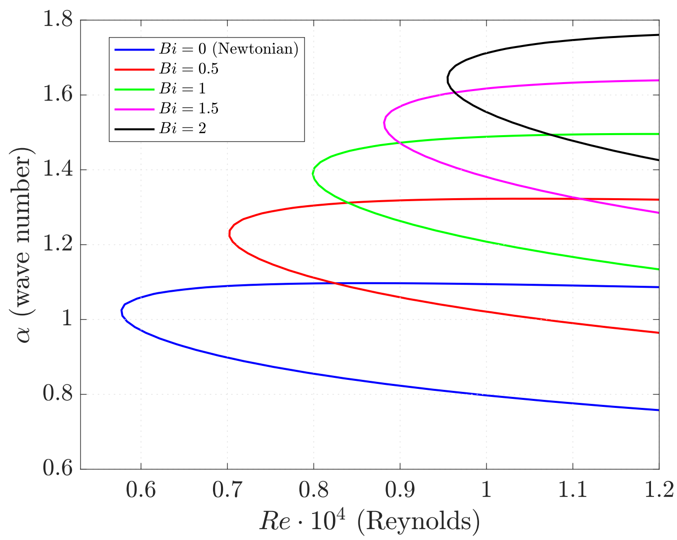

Figure 4: Neutral stability curves fo the Bingham model with fixed Bi and Re independent.

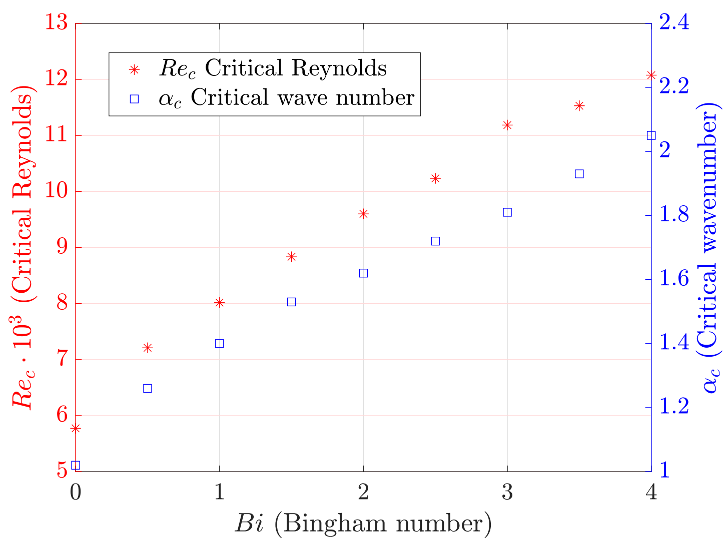

Figure 5: Critical Reynolds and wave number for the Bingham model with Bi and Re independent.

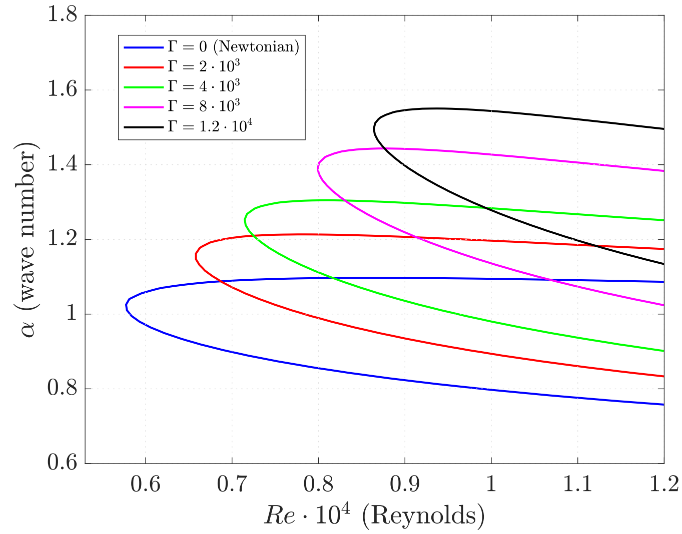

Figure 6: Neutral stability curves: Bingham model with fixed Γ.

Fig. 4 displays the neutral stability curves for different (fixed) values of the Bingham number Bi. Consistently with the results of [7] we find that the increase of the Bingham number has a stabilizing effect as the critical Reynolds number increases as Bi increases. The blue curve, corresponding to $Bi = 0$, represents the neutral stability curve in the Newtonian case.

In Fig. 5 we report the critical Reynolds number and the corresponding critical wave number for different values of Bi. In accordance with the results in [7] we see that the critical conditions increase almost linearly with the Bingham number.

Fig. 6 displays instead the neutral stability curves for different values of the dimensionless number Γ, that is the Bingham and Reynolds number are not considered to be independent but related through (26). In practical applications Γ is of order $O(10^3)$ to $O(10^5)$ (table 1).

Finally, in Fig. 7 we report the critical Reynolds number and the critical wave number for different values of Γ. As in the case in which the Bingham and Reynolds numbers are considered to be independent from each other, Re_{cr} and

Table 1: Material parameters for mud and blood.

Fluid	τ_0^* (Pa)	ϱ^* (Kg/m^3)	L^* (m)	μ^* (Pa$\cdot$ s)	Γ
Mud	2	1910	4	0.1	$6.11 \cdot 10^5$
Blood	0.5	1000	10^{-2}	$3 \cdot 10^{-3}$	$5.5 \cdot 10^3$

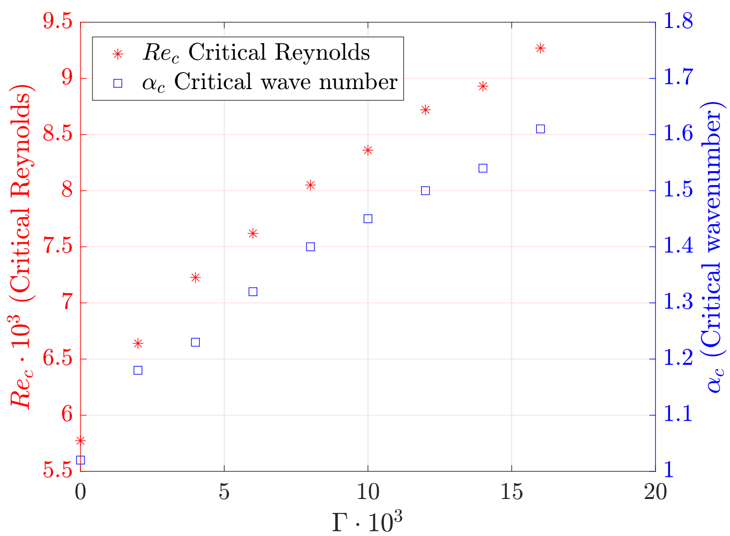

Figure 7: Critical Reynolds and wave number: Bingham model with Bi and Re dependent.

α_{cr} depends almost linearly on Γ.

4.2. Regularized models

On using the same numerical approach as for the Bingham model, we solve the eigenvalue problem (30) and (31) with $o = S, P$.

Figs 8 and 9 display the neutral stability curves obtained using the models due to Allouche et al. [1] and Papanastasiou [14] under the assumption that Bi and Re are independent. The parameter ε is set equal to 10^{-3}, so that the discrepancy between the basic Bingham and the basic regularized solution is of order $\leqslant O(10^{-3})$ (see figs 2 and 3). Smaller values of ε can also be considered, but this requires a larger number of Gauss-Lobatto points (we would need more

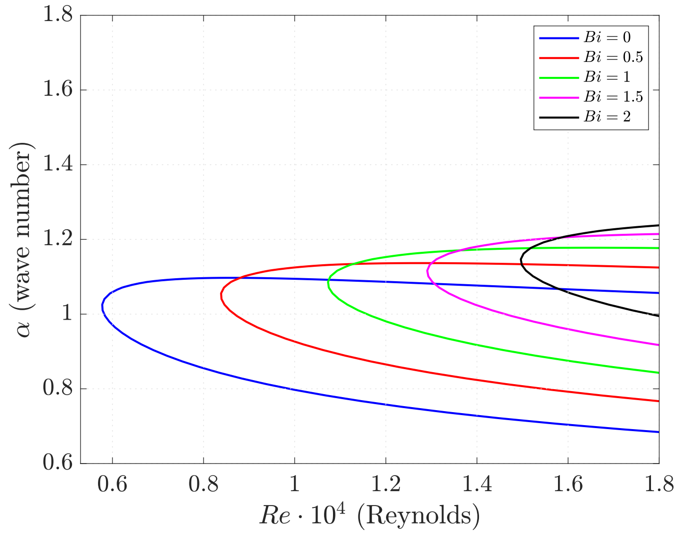

Figure 8: Neutral stability curves for the simple model with Bi and Re independent from each other. The dimensionless parameter ε is set equal to 10^{-3}.

than 600 Gauss-Lobatto points for $\varepsilon = 10^{-4}$) on which one has to discretize the eigenvalue problem . We observe that the critical Reynolds and wave numbers when using the regularized model differ substantially from those obtained for the 'exact' Bingham model (see also [8]). On the other hand, we observe that the discrepancy of the critical conditions between the simple (Fig. 8) and Papanastasiou models (Fig. 9) is negligible for $\varepsilon = 10^{-3}$. Indeed, as shown in Fig. 10, the critical Reynolds and wave numbers for the simple and Papanastasiou models differs by less than 1% when Re and Bi are assumed to be independent.

Figures 11 and 12 display the neutral stability curves for the simple and Papanastasiou models when keeping Γ fixed, i.e. assuming that Bi and Re are related through (26). We take again $\varepsilon = 10^{-3}$ and we find that the critical conditions for the simple and Papanastasiou models are essentially the same (the discrepancy is again less than 1%). We notice that, also for the case in which Bi and Re are dependent, these critical conditions are substantially different from those obtained for the Bingham model (Fig. 6).

To quantify the deviation of the critical numbers for the regularized models

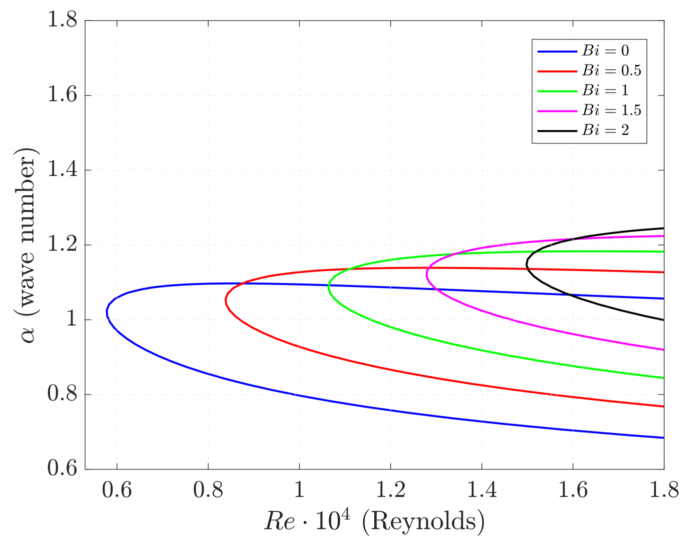

Figure 9: Neutral stability curves for the Papanastasiou model with Bi and Re independent from each other. The dimensionless parameter ε is set equal to 10^{-3}.

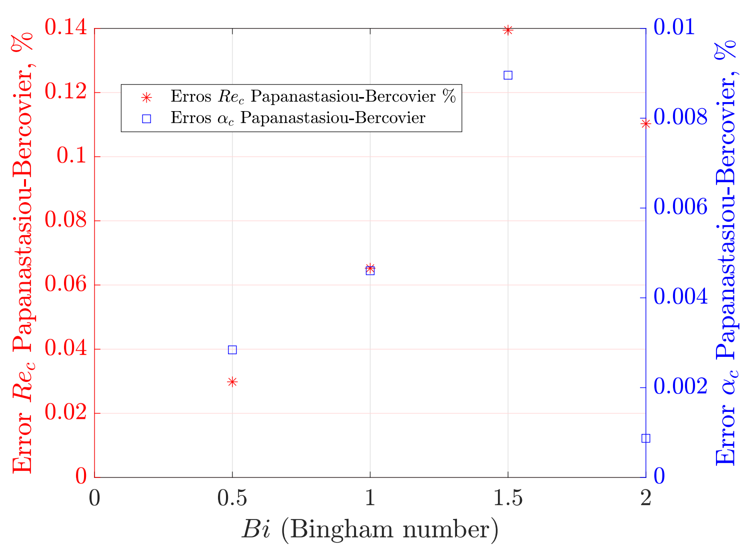

Figure 10: Difference (%) in the critical Reynolds and wave numbers when using the Bercovier and Papanastasiou models for $\varepsilon = 10^{-3}$ and Bi and Re independent from each other.

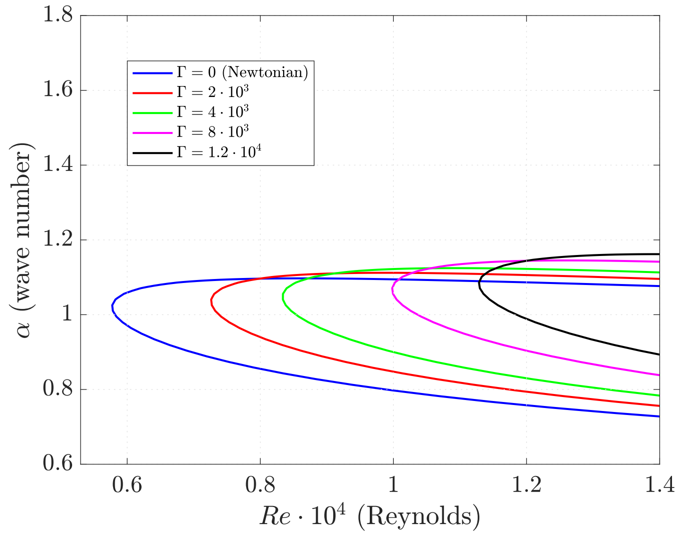

Figure 11: Neutral stability curves for the simple model with Γ fixed and $\varepsilon = 10^{-3}$.

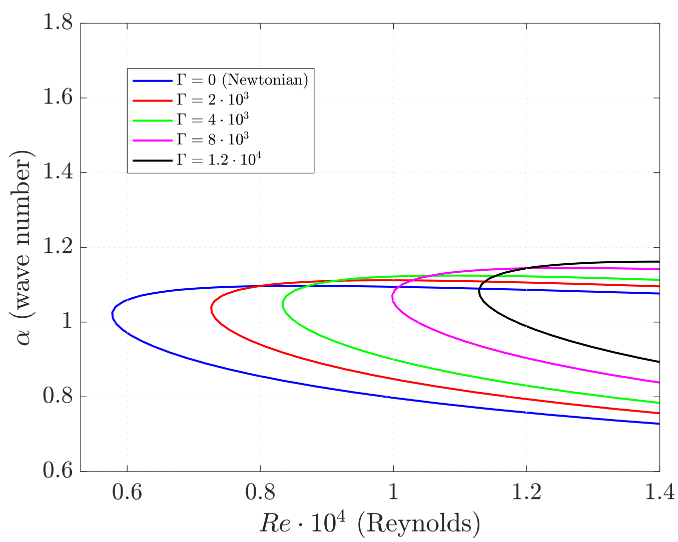

Figure 12: Neutral stability curves for the Papanastasiou model with Γ fixed and $\varepsilon = 10^{-3}$.

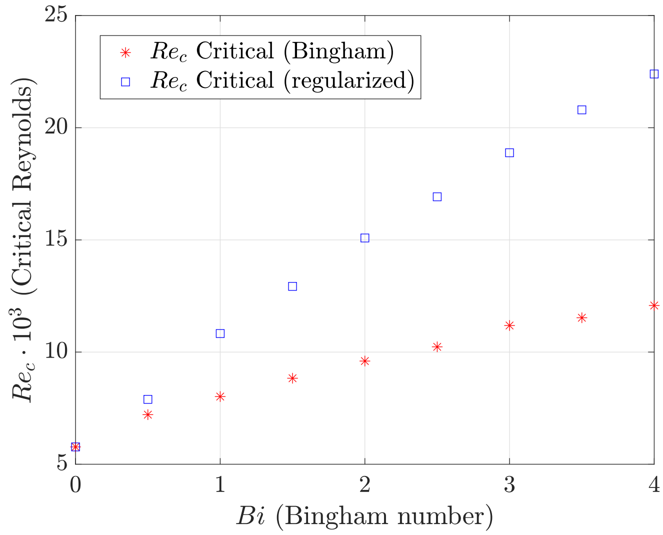

Figure 13: Re_c vs Bi: Bingham and regularized with $\varepsilon = 10^{-3}$ and Re and Bi independent.

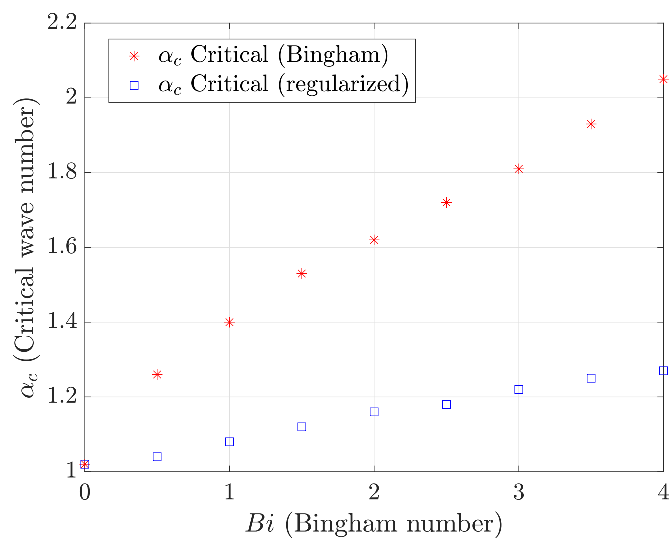

Figure 14: α_c vs Bi: Bingham and regularized with $\varepsilon = 10^{-3}$ and Re and Bi independent.

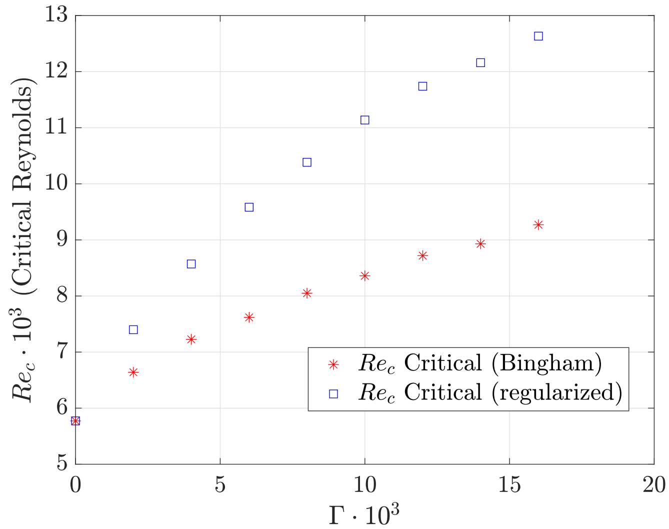

Figure 15: Re_c vs Γ: Bingham and regularized with $\varepsilon = 10^{-3}$ and Re and Bi dependent.

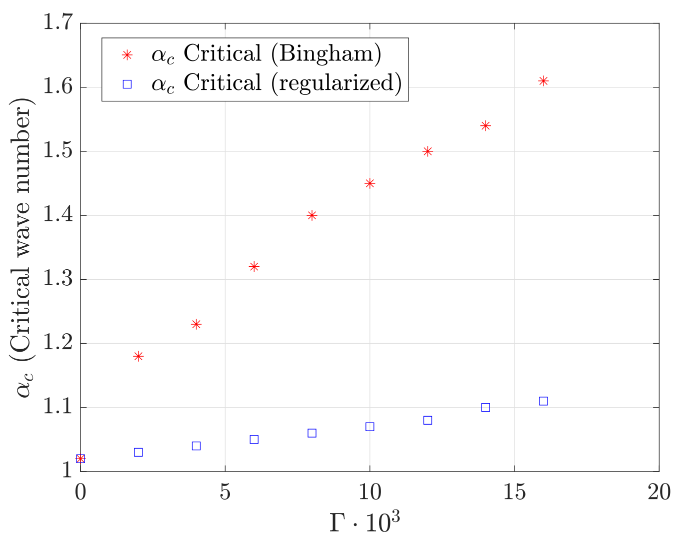

Figure 16: α_c vs Γ: Bingham and regularized with $\varepsilon = 10^{-3}$ and Re and Bi dependent.

from those of the Bingham model we plot Re_c and α_c with Bi and Re independent (Figs 13, 14) and with Bi and Re related through (26) (Figs 15, 16). We see that the discrepancy increases linearly with the Bingham number or Γ. In the next subsection we shall show that the difference in the critical conditions of the Bingham and approximating models are essentially due to the fact that when using the Bingham model, a portion of the fluid (the unyielded domain) does not dissipate energy because of its rigidity.

4.3. Regularized model without the inner core

In the Bingham model the domain of the evolution equation of perturbation is

$$\Omega = [-1, -s_B] \cup [s_B, 1],$$

since the core, being rigid, remains unperturbed. The regularized models act instead on the whole domain $[-1, 1]$. Here, we show that the discrepancy in the critical conditions between the exact Bingham model and the regularized models is due to the different domains in which the disturbances act.

To prove our assertion we observe that, for a sufficiently small ε, we may consider the disturbance equation (30) only in the domain Ω, thus excluding the effects of the perturbations in the domain $[-s_B, s_B]$. As for the Bingham case the domain Ω has to be mapped into $[-1, 1]$. To this aim we consider again the change of variable (38). With this change of variables, equation (30) (with $o = S, P$) becomes

$$\begin{aligned}
&\Big\{\bar{h}_o \lambda^4 \mathcal{D}^4 + \lambda^4 (2\mathcal{D}\bar{h}_o)\mathcal{D}^3 \qquad (42)\\
&+ \left[2\alpha^2(\bar{h}_o - \bar{g}_o) + \lambda^2 \mathcal{D}^2 \bar{h}_o + i\alpha Re(c - \bar{u}_o)\right]\lambda^2\mathcal{D}^2 + 2\alpha^2\lambda^2(\mathcal{D}\bar{h}_o - \mathcal{D}\bar{g}_o')\mathcal{D}\\
&+ i\alpha^3 Re(\bar{u}_o - c) + \alpha^2(\lambda^2\mathcal{D}^2\bar{h}_o + \alpha^2\bar{h}_o) + i\alpha Re\lambda^2\mathcal{D}^2\bar{u}_o\Big\}\bar{v} = 0,
\end{aligned}$$

where

$$\bar{u}_o(\eta) = u_o(\bar{\eta}^{-1}(\eta)), \quad \bar{g}_o(\eta) = g_o(\bar{\eta}^{-1}(\eta)), \quad \bar{h}_o(\eta) = h_o(y\left(\bar{\eta}^{-1}(\eta)\right). \qquad (43)$$

In Fig. 17 we show the neutral stability curves obtained by solving (42) for the simple simple model with $\varepsilon = 10^{-3}$. The Papanastasiou model provides

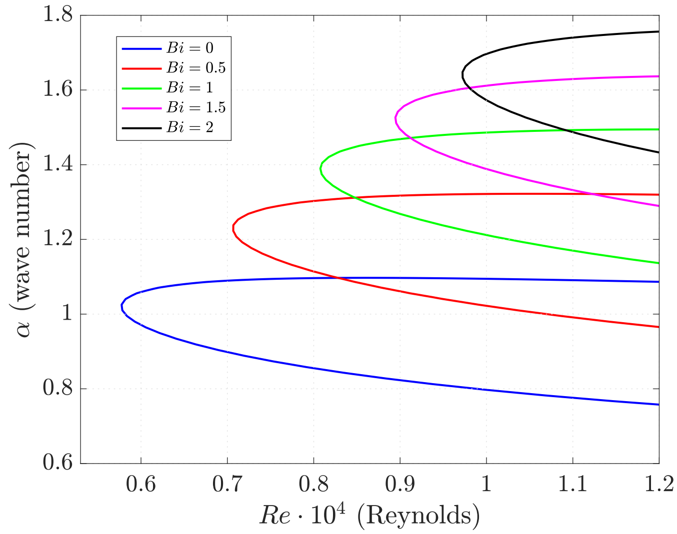

Figure 17: Neutral stability curves for the simple model with unperturbed inner region $[-s_B, s_B]$, and Bi and Re independent from each other. $\varepsilon = 10^{-3}$.

essentially the same results. As one can see, the neutral curves practically coincides with those obtained for the Bingham model (see Fig. 4). This proves that the discrepancy between the regularized models and the Bingham model is entirely due to the perturbation effects that develop in the region $[-s_B, s_B]$. When using the Bingham model, this region represents the rigid core which does not dissipate energy. On the contrary, when one uses a regularised model energy is dissipated throughout the domain and this explains the fact that the critical Reynolds number for the Bingham model is less than the one for a regularised model.

5. Conclusions

We have focussed on the stability of Poiseuille flows in a viscoplastic fluid by considering three different rheological model: the classical Bingham model and two smoothed models (simple and Papanastasiou). The purpose of this article is in fact to investigate, “ceteris paribus”, the differences between these three models in predicting the onset of instability of the basic flow. We have shown that the critical conditions marking the transition to instability when using the Bingham model do not coincide with those of the two regularized models (which, instead, give the same critical thresholds). This discrepancy depends on the rigidity of the Bingham inner core. Indeed, the regularized models allow energy dissipation throughout the channel, which is not the case in the Bingham model. To justify our claim we have re-examined the stability of Poiseuille flows by removing the region corresponding to the unyielded phase when using the Bingham model, and obtained that, with this truncation, the simple and Papanastasiou models give the same critical thresholds as those predicted by the Bingham model.

Acknowledgments

This research was partially supported by GNFM of Italian INDAM.

References

[1] Allouche M., Frigaard I.A., Sona G., Static wall layers in the displacement of two visco-plastic fluids in a plane channel, J. Fluid Mech., 424 (2000), 243–277.

[2] Bercovier M., Engelman M., A finite-element method for incompressible non-Newtonian flows, J. Comp. Phys., 36 (1980), 313–326.

[3] Huilgol R.R., Fluid Mechanics of Viscoplasticity, Springer (2016).

[4] Farina A., Fusi L., Viscoplastic Fluids: Mathematical Modeling and Applications. In: Farina A., Mikelić A., Rosso F. (eds) Non-Newtonian Fluid Mechanics and Complex Flows. Lecture Notes in Mathematics, 2212 (2018). Springer, Cham.

[5] L. Fusi, Farina A., Rosso F., On the mathematical paradoxes for the flow of a viscoplastic film down an inclined surface, International Journal of Non-Linear Mechanics, 58, (2014), 139–150.

[6] Fusi L., Farina A., Rosso F., Roscani S., Pressure driven lubrication flow of a Bingham fluid in a channel: a novel approach, Journal of Non-Newtonian fluid mechanics, 22, (2015), 66-75.

[7] Frigaard I.A., Howison S.D., Sobey I.J., On the stability of Poiseuille flow of a Bingham fluid, J. Fluid. Mech., 263, (1994), 133–150.

[8] Frigaard I.A., Nouar C., On the usage of viscosity regularisation methods for visco-plastic fluid flow computation, J. Non-Newtonian Fluid Mech., 127, (2005), 1–26.

[9] Garimella S. M., Anand M., Rajagopal, K. R., A New Model to Describe the Response of a Class of Seemingly Viscoplastic Materials, Applications of Mathematics, (2021), 1-13.

[10] Pitsillou R., Georgiou G.C., Huilgol R.R., On the use of the Lambert function in solving non-Newtonian flow problems, Phys. of Fluids, 32, 093101 (2020).

[11] Métivier C., Nouar C., Stability of a Rayleigh-Bénard Poiseuille flow for yield stress fluids-Comparison between Bingham and regularized models, Int. J. Non-Lin. Mech., 46, (2011), 1205–1212.

[12] Rajagopal K.R., Srinivasa A.R., On the thermodynamics of fluids with implicit constitutive relations, ZAMP, 59, (2009), 715–729.

[13] Rajagopal K.R., On the Flows of Fluids Defined through Implicit Constitutive Relations between the Stress and the Symmetric Part of the Velocity Gradient, Fluids, 1,5, (2016), 1020005.

[14] Papanastasiou T.C., Flows of materials with yield, J. Rheol., 31 (5), (1987), 385–404.